Lake Carbonate Geochemistry as a Proxy for Paleohydrology: A Validation-in-Time at West Basin Lake, Victoria

Thesis submitted in accordance with the requirements of the University of Adelaide for an Honours Degree in Environmental Geoscience

Chloe Elizabeth Dean

November 2019

THE UNIVERSITY of ADELAIDE

LAKE CARBONATE GEOCHEMISTRY AS A PROXY FOR PALEOHYDROLOGY: A VALIDATION-IN-TIME AT WEST BASIN LAKE, VICTORIA

ABSTRACT

There is a lack of extensive historical climate data in Australia, meaning high-resolution paleoclimate studies are essential for a more comprehensive understanding of natural climate variability. The majority of paleohydrology records in the south-eastern Australia region are low resolution, millennial time-scale reconstructions, resulting in a lack of understanding of climate variability at shorter time-scales, relevant to human life spans. Here, we attempt to validate the use of geochemical analysis of lake sediments from West Basin, Victoria, as a way to create a high resolution paleohydrology reconstruction. The isotopic composition of the lake water in West Basin is primarily controlled by the precipitation to evaporation ratio (P:E). Ostracod calcite and bulk inorganic carbonates (BIC) that form within the water column reflect these changes and thus, are used as proxies of past changes in P:E. This reconstruction is supported by a ^{210}Pb- and $^{240/230}$Pu-based chronology which estimates a sediment accumulation rate of 0.3 to 0.4 cm/year and a maximum age at 40 cm of 118 years. This enables the resulting oxygen and carbon profiles to be validated against instrumental records of annual rainfall and temperature. The oxygen profile exhibits good agreement with this climate record, with peaks in δ^{18}O values often coinciding with periods of low annual rainfall. Based on this, the ostracod record was determined to be capable of recording reliable, high resolution changes in P:E. The BIC record, though less consistent, can produce a detailed profile where ostracods are unavailable. Studies of this kind are vital to improving the accuracy of proxy system models which allow for reconstructions to be extended further in the geological record. Such models would allow for contextual understanding of the severity of drought occurrences and the assessment of the possible impacts of human induced climate change.

KEYWORDS

Geochemistry, paleohydrology, lake sediments, Ostracod calcite, bulk inorganic carbonate.

TABLE OF CONTENTS

LIST OF FIGURES AND TABLES

1.0 INTRODUCTION

Droughts are a common occurrence in Australia, with weather systems naturally cycling through droughts and periods of increased rainfall, as a result of large scale ocean-atmosphere systems such as El Nino Southern Oscillation (ENSO), the Indian Ocean Dipole (IOD) and the Southern Annular Mode (SAM) (Braganza, Gergis, Power, Risbey, & Fowler, 2009; Ummenhofer et al., 2009). Australia has experienced ten major droughts since records began, and many other smaller regional droughts in its history (Australian Bureau of Statistics, 2012). Droughts in Australia have far reaching economic and ecological effects, with the most recent major drought event, the Millennium Drought (1997 to 2009), causing extensive water shortages, crop losses and the drying of river systems (Nicholls & Kariko, 1993; Risbey, Pook, McIntosh, Ummenhofer, & Meyers, 2009; Ummenhofer et al., 2009). Much has been done to understand the modern hydrology of the Australian continent on various scales (Feng, Li, Li, Zhu, & Xie, 2015; Pui, Sharma, Santoso, & Westra, 2012; Ummenhofer et al., 2009) with the effects of the SAM, ENSO and the IOD on precipitation events now relatively well understood, for short time scales, though they remain elusive over longer timescales of decades to centuries.

Understanding the extent and causes of these past decadal to centennial drought occurrences is fundamental to our ability to manage water systems and to mitigate the effects of these events (Pui et al., 2012). Such understanding is particularly relevant as temperatures continue to increase as a result of human induced climate change (Braganza et al., 2009; Nicholls & Kariko, 1993). Paleoclimate studies are of particular importance in Australia due to the limited length and quality of instrumental and

historical data available (Braganza et al., 2009; Wilkins, Gouramanis, De Deckker, Fifield, & Olley, 2013). It is not yet certain if, or what effect increased temperatures over the world's oceans have on the climate systems that govern rainfall over Australia, because the drivers of these phenomena are so complex (Braganza et al., 2009; Nicholls & Kariko, 1993; Pui et al., 2012; Risbey et al., 2009). In order to determine the changes in these patterns that are a result of human induced climate change, their historical effects need to be investigated via robust, high resolution paleoclimate reconstructions (Braganza et al., 2009). Doing so will greatly aid in our understanding of Australia's drought history, and allow current events to be placed in a historical context.

Lakes and lake sediments are highly sensitive to climatic and hydrological change, making them excellent sources of paleoclimatological data (Steinman & Abbott, 2013). Lake sediments provide continuous, high resolution cores that contain a multitude of proxies, which can be used to investigate for climatic and hydrological change (Steinman & Abbott, 2013). Furthermore, lakes exist in all sorts of environments globally, and therefore are able to record almost all types of climate systems, creating a vast wealth of studies upon which to draw when investigating similar climates and environments around the world (Gouramanis, Wilkins, & De Deckker, 2010; Last & De Deckker, 1990; Mischke et al., 2010; Steinman, Rosenmeier, Abbott, & Bain, 2010). However, the sensitivity to environmental changes that makes lakes such an attractive source of paleoclimate data, is also a source of uncertainty in the field of paleolimnology (Steinman & Abbott, 2013; Steinman et al., 2010). Lakes are complex systems that take into account the effects of geology, temperature, groundwater, rainfall and ecology, among others (Steinman & Abbott, 2013). This means that paleoclimate

signals are often a mixture of these inputs and as a result, quantifying climate from lake sedimentary data proves a significant challenge (Steinman & Abbott, 2013).

A study by Bowler and Tatsuji (1971) was one of the first to highlight the usefulness of Australia's saline lakes as a valuable source of paleoclimatic data. As a result, the Newer Volcanics Region of Western Victoria has attracted many more studies since, resulting in a comprehensive understanding of this region's hydrological changes during the Holocene (Bowler, 1981; De Deckker, 1986; Gell, Barker, De Deckker, Last, & Jelicic, 1994; Gouramanis, De Deckker, Switzer, & Wilkins, 2013; Last & De Deckker, 1990; Wilkins et al., 2013). However, these studies are limited in their resolution, and have largely focussed on low frequency changes over a longer, centennial-millennial timescale and for the most part, have not attempted to quantify the changes in hydrology. Oxygen isotopes provide a potential means to quantify hydrological change, (Steinman, Abbott, Mann, Stansell, & Finney, 2012) were able to quantitatively reconstruct precipitation over 1500 years based on the oxygen isotopic record of lake sediments from the Pacific Northwest USA. Such an approach has been applied to lakes in Australia, though at low temporal resolution (Gouramanis et al., 2010; Wilkins et al., 2013). Despite these studies and strong theoretical grounding, there's still uncertainty as to the degree to which oxygen isotope geochemistry can be used to quantify past climates. Few studies worldwide have attempted to compare oxygen isotope records against climate data, largely due to the challenge of obtaining high resolution isotope profiles from sediment records that span the instrumental period. One of few exceptions to this, is the study conducted by Dean et al. (2015) where 17 years of lake monitoring

was used as a basis against which to determine how different proxies within the lake responded to the recorded changes. A similar approach is taken in this study.

This study aims to investigate the validity of using ostracod calcite and bulk inorganic carbonate (BIC) to reconstruct the temperature and oxygen isotopic composition of lake water, and hence the precipitation/evaporation ratio (P:E) of West Basin Lake. This will be achieved by comparison of isotopic analysis of lake sediments with instrumental climate data for the last ~115 years. Ostracods, also known as 'seed shrimp', were chosen as a proxy for this study as they are abundant organisms that have been shown to be present throughout the sediment record in many lakes globally (Fedotov, Ignat'ev, & Velivetskaya, 2015; Marchegiano, Francke, Gliozzi, & Ariztegui, 2018), and in Australia (De Deckker, 1986; Gell et al., 1994). Ostracods are useful proxies, sampling oxygen and carbon directly from the lake water in order to build their low-magnesium calcite shells, therefore recording any changes within the lake isotopic composition (Decrouy, Vennemann, & Ariztegui, 2011; Gouramanis et al., 2010). Ostracods have been extensively studied globally, with many species being well documented proxies for lake isotopic composition (Gouramanis et al., 2010; McCormack, Viehberg, Akdemir, Immenhauser, & Kwiecien, 2019). Trace element analysis and species based transfer functions are also commonly used to infer other parameters, such as temperature and the salinity of lake waters (Börner et al., 2013; Gouramanis et al., 2010; Zhu, Chen, Li, Ren, & Liu, 2012). A more technically simple approach is also taken in this study, the $\delta^{18}O$ and $\delta^{13}C$ of bulk inorganic carbonates (BIC) are analysed against climate data. BIC is the portion of the bulk sediment that consists of fine grained inorganic carbonates. The use of BIC allows for a comprehensive record to be

constructed, as sample collection and preparation is simple and time efficient in comparison to that of Ostracods.

In order to make an assessment of the validity of these analyses, an accurate and high resolution sediment age model that spans the period of instrumental climate data collection is required. Sediment dating that covers this period, relies heavily on the use of ^{210}Pb decay models as well as the relatively new technique, involving $^{239+240}$Pu spikes. ^{210}Pb dating is based on the principle that ^{210}Pb decays at a constant rate, and therefore decreases in activity down the sediment core (Appleby & Oldfield, 1978). ^{210}Pb is a radioactive lead isotope with a half-life of 22.26 years and thus will produce a relatively reliable down-core chronology for recent sediments, spanning back approximately 111 years, or 5 half-lives (Appleby & Oldfield, 1978). This method uses two models which rely on the assumptions of either a constant rate of supply (CRS) of ^{210}Pb from the atmosphere, or else a constant initial concentration (CIC) of ^{210}Pb (Zhang, Zhang, Garbrecht, & Steiner, 2015). A detailed explanation of the processes involved can be found in (Appleby & Oldfield, 1978). Plutonium radioisotope dating relies on the presence in sediments of $^{239+240}$Pu isotopes resulting from nuclear bomb testing in 1963 (Bollhöfer et al., 1994). Pu dating, therefore is achieved by testing for the total amount of $^{239+240}$Pu, as well as the ratio of these two isotopes (Bollhöfer et al., 1994). As such, the $^{239+240}$Pu peak (which represents sediments from 1963) is used as a horizon against which to check the validity of the results of ^{210}Pb dating (Bollhöfer et al., 1994). Sanders et al. (2016) demonstrated the usefulness of both these techniques within the same core by examining ^{210}Pb data against additional $^{239+240}$Pu ages. Such studies validate the use of ^{210}Pb and others to create age models. As such, it is the aim

of this project to combine ^{210}Pb and $^{239+240}Pu$ in combination with radiocarbon models to conduct a fine resolution age/depth analysis in order to accurately constrain the data from the proxy record within West Basin Lake.

This study aims to test the validity of oxygen isotopes from both Ostracods and BIC as proxies for past P:E changes. It is thought that if the oxygen isotope trend is able to correlate to known drought occurrences in recent history, then this method could potentially be used to extrapolate further throughout the Holocene. An improved understanding of drought frequency in Australia has the potential to aid in drought and water resource management, and prepare us for future drought events. Such a study will add to the growing understanding of drought variability and its drivers, thereby informing on the effects of future drought events in region. This is a vital area of study as it is key to preserving the viability of agricultural production (Risbey, Pook, McIntosh, Wheeler, & Hendon, 2009) and ensuring the environmental health of southeastern Australia.

2.0 BACKGROUND

2.1 Drought in Australia

Australia, as a whole has suffered through many droughts since records began, the largest of which are the Federation Drought (1895-1903), the World War II Drought (1939-1945) and the Millennium Drought (1997-2009) (Freund, Henley, Karoly, Allen, & Baker, 2017; Ummenhofer et al., 2009). There are also several historical records of droughts during the early periods of European settlement, these being the Settlement Drought (1790-1793), Sturt's Drought (1809-1830) and the Goyder Line Drought

(1861-1866) (Freund et al., 2017). Understanding the extent and drivers of past drought occurrences is fundamental to placing modern drought periods into context. However, the instrumental record of rainfall and drought periods is limited in its ability to place modern droughts into longer term context, resulting in a gap in the knowledge of long term climate trends, and our ability to model droughts that exceed the timeframe of instrumental data. Therefore, other longer term records must be analysed to clarify understanding of the causes and effects of drought. This can be done by investigating past climatic changes recorded by various proxies in the geological record.

2.2 Australian Paleoclimate Research

A limiting factor for Australian paleoclimatic studies is the sparsity of paleoclimate records (Barr et al., 2014; O'Donnell, Cook, Palmer, Turney, & Grierson, 2018) and the large variation in hydrology across the continent (Gouramanis et al., 2013; Ummenhofer et al., 2009). Much of the current work in paleoclimatology in Australia is based on coral, tree rings and lake sediments as proxies for past temperature and hydrology, with the majority of work focussed on the Eastern Coast (O'Donnell et al., 2018). It has been demonstrated that tree rings offer good insight into drought variability for the western section of the continent, with (O'Donnell et al., 2018) highlighting the potential for construction of a drought atlas from such records. With recent work focussing on the improvement of the potential uses of tree ring data and the compilation of data sets spanning millennia (Esper et al., 2016), such drought atlases may be possible with further research. Improvements in paleoclimate data collected from corals is being made within Australia. A study by (Sadler, Nguyen, Leonard, Webb, & Nothdurft, 2016) identified the potential for the use of a new species of coral, *Acropora,* for paleoclimate

reconstruction, showing that this species can be used to identify "greater seasonal amplitude" in paleotemperature reconstructions.

2.3 Regional Paleoclimate Studies

Lake sediments provide continuous, long term records of paleoclimates and hydrology. Which are therefore powerful tools to investigate longer term trends in Australian climate. Previous study in the region of South Eastern Australia has largely focussed on lake level variability as an indicator of changes in the hydrological cycle over the Holocene (Bowler, 1981; Bowler & Tatsuji, 1971; Gell et al., 1994; Last & De Deckker, 1990; Wilkins et al., 2013). As a result, the Holocene history of the area is well understood, adding much to the understanding of the variability of Australian climate (Wilkins et al., 2013). Bowler (1981) studied sediment type and texture, morphology and pollen from Lake Keilambete to produce a thorough paleoclimatic reconstruction and infer lake levels. The lake level fluctuations determined by Bowler (1981) were based largely on grain size analysis and the presence and disappearance of carbonates and ooids. The results of this study showed a marked increase in lake levels in the early/mid Holocene (approx. 7.8 to 6.2ka), followed by a decline around 3.3 ka, with a subsequent rise and a final decline around the time of European Settlement Bowler (1981). Further research based on Bowler's work was conducted by Wilkins et al. (2013) in which higher resolution analysis of Lake Keilambete and Gnotuk was undertaken in order to test the lake level curve constructed by (Bowler, 1981). This study supported the previous work, while adding that higher resolution was able to determine more precise dates for lake level changes, as well as determining a correlation between temperature changes and precipitation in the region (Wilkins et al., 2013).

Although the area is well studied, there is still need for the development and assessment of higher resolution techniques to analyse paleoclimate on a finer timescale. A high-resolution study conducted on Lake Surprise and Elingamite by Barr et al. (2014) used diatom conductivity as a proxy for lake level changes to infer drought occurrences in the region, also demonstrated good agreement with the previously mentioned studies. (Barr et al., 2014) showed potential for more extreme droughts than have yet been seen, based on the record produced. Many studies that have previously investigated the paleohydrology of the region are at much coarser time scales than (Barr et al., 2014), and/or unable to quantify the observed changes. This highlights the need for further, detailed research into the drought history of Australia, which will allow for quantitative assessments on finer time-scales. It is the aim of this project to fulfil part of that need.

2.4 Paleoclimate Models

One approach for obtaining quantitative data from lake sediments is to compare lake isotope data is with models of the lake hydrology and geochemistry, known as the 'proxy system model' approach. Steinman et al. (2010) conducted an assessment of two small closed basin, crater lakes, in order to examine the various climatic controls on hydrology and isotope variability within such lakes. From this, it was determined that increased out-seepage rates and surface area to volume ratio changes made lakes more sensitive to climate fluctuations and therefore act as good records of precipitation changes (Steinman et al., 2010). Further assessments by Steinman and Abbott (2013) were able to verify that "quantitative interpretations of lake sediment $\delta^{18}O$ records are attainable", by showing a strong correlation between $\delta^{18}O$ of water samples from the study area and rainfall using a Monte Carlo ensemble. Carbonate $\delta^{18}O$ in lakes across the USA have also been used to create a basic grid model of past regional rainfall

variability within that region, with the potential for expansion into a global model (Jones & Dee, 2018). These models rely on well-established proxy to climate relationships in order to build and improve upon such models, which is what studies such as this one aim to achieve.

2.5 West Basin Lake Background and Site Description

West Basin is a hypersaline, meromictic volcanic maar lake, with a maximum depth of 13.5 m (Gell et al., 1994).It is located approximately 150 km west of Melbourne, in the Western Victoria Plains (Figure 1) (Last & De Decker, 1990). The climate in the region is temperate, with a mean maximum temperature of 18.5 ºC and mean annual rainfall of 534 mm (Bureau of Meteorology, 2019). Much of the Western Victoria Plains are comprised of Quaternary basalts, with volcanic cones forming the basins for many lakes in the area (Last & De Decker, 1990). The lakes in this region are thought to lie above regional groundwater sources, and therefore have a hydrological input that is largely meteoric in origin (Last & De Decker, 1990).

West Basin Lake has been the focus of several studies which have examined the sedimentological and microfossil content of the sediments (Gell et al., 1994; Last & De Deckker, 1990). Last and De Decker (1990) analysed the carbonate content of West Basin and its neighbour, East Basin, and determined the majority of the carbonate in both lakes was formed via precipitation in the water column and in the sediment-water interface. The carbonate identified in the two lakes varied in species (largely from dolomite to calcite with lesser hydromagnesite and magnesite) and abundance through time, indicative of changes in climate and hydrological characteristics of the lake

throughout the Holocene (Last & De Deckker, 1990). A more detailed study conducted by Gell et al. (1994) determined climatic influences on the lake's hydrology over the last 10,000 years, confirming the earlier conclusions by (Last & De Deckker, 1990). Gell et al (1994) described the diatom, ostracod and pollen composition of the within West Basin sediments and from this, reconstructed salinity changes, as a function of lake level. This study was able to verify the work by Last & De Decker (1990) with the same changes in lake level determined from the various proxies (Gell et al., 1994). However, there are still major questions about the relationship between climatic change and its expression in the geochemistry of the sediments.

West Basin Lake was chosen as the site for this study, as it satisfies the parameters outlined by Steinman and Abbott (2013) for a lake to represent a 'paleo-rain gauge'. For a lake to qualify, the majority of the water input is derived from direct precipitation and therefore the isotopic composition of the lake is controlled largely by the P:E (Timms, 1972). Previous studies that have determined the sediment is fast accumulating, laminated and undergoes little disturbance or bioturbation, making it a great site for the potential of a continuous, high resolution paleohydrological reconstruction (Gell et al., 1994; Last & De Deckker, 1990; Lockier, 2015; Prodan, 2014). This work in this study, builds upon previous work that has been conducted in this region, and adds new insight into the geochemical processes that are governed by changes in climate.

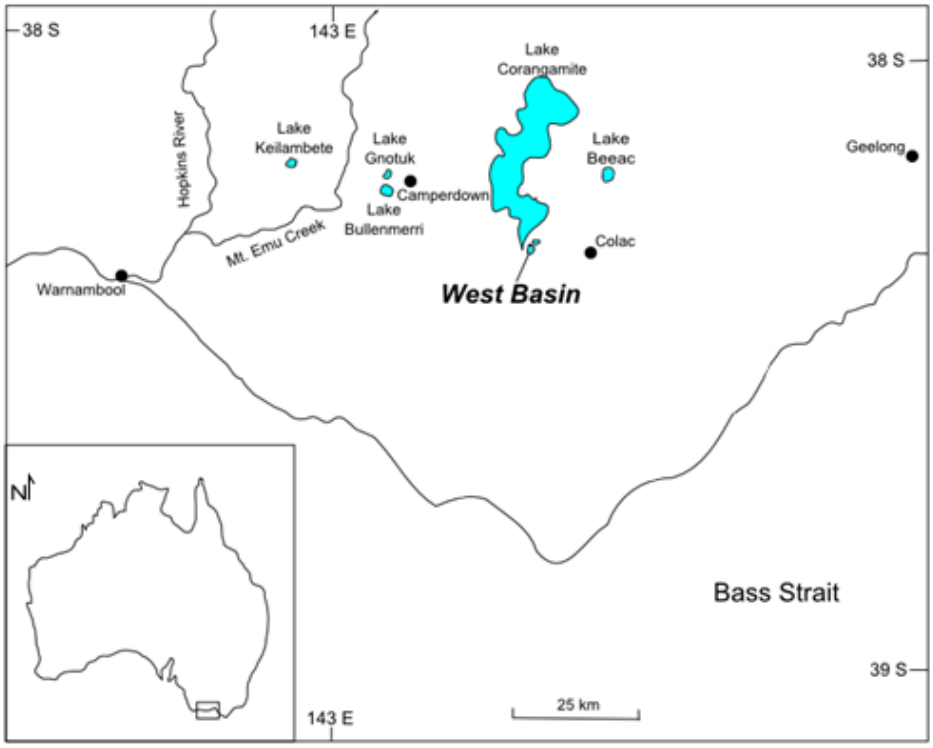

Figure 1. Map showing location of West Basin Lake and other lakes in the region (blue) in relation to Australia and regional towns (black). Map adapted from Gell et al (1994).

3.0 METHODS

3.1 Coring and Subsampling

Two sediment cores were examined in this study, the first 4 metre core WB86-2 was taken from West Basin in 1986 using a Mackereth corer, subsampled at 0.5 cm intervals and stored at the Australian National University at 4 ºC by Last and De Decker (1990). The second 40 cm core also originated from West Basin in 2015 using a Pylonex HTH gravity corer, with the core taken from the deepest centre of the lake. This corer extruded sediment in increments which were sliced off and stored at Adelaide University at 4 ºC until analysis. The first 20 cm of this core was subsampled every 0.25 cm, and the remaining 20 cm was subsampled every 0.5 cm. The sampling location of both cores is shown in Figure 2 below.

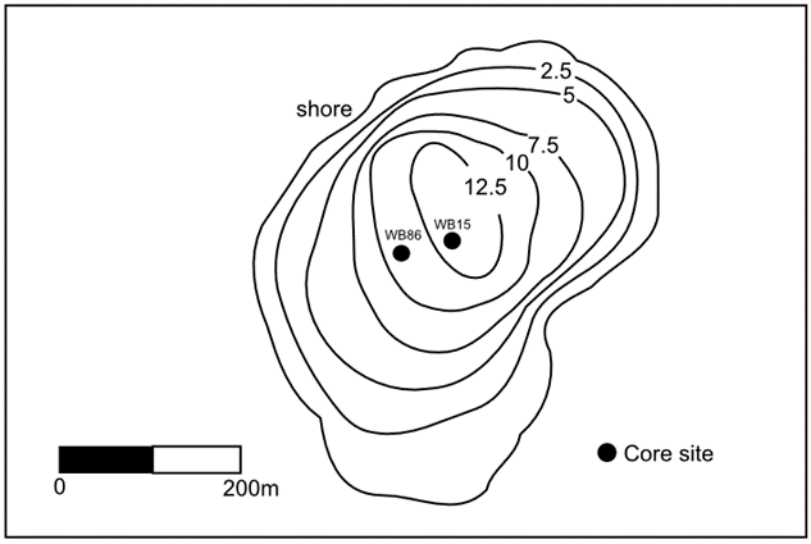

Figure 2. Bathymetric map of West Basin Lake, showing coring sites for WB15 and WB86-2, used in this study. Map adapted from Gell et al (1994).

3.2 Sediment Dating

Sediment chronologies for the last ~115 years were developed using ^{210}Pb and plutonium radioisotopes at the Australian Nuclear Science and Technology Organisation (ANSTO). Detailed description of the protocols for sample preparation are given in Appendix A.

An initial lead profile was established for the intervals between 0.25 cm and 36.0 cm by isolating polonium (Po) and radium (Ra) from samples (Appendices B and C). Further lead dating was undertaken in 2019 following the same protocols for a further four sample depths (3.0-3.25 cm, 8.5-8.75 cm, 13.0-13.25 cm and 22.0-22.5 cm). Isolated Po samples were loaded into the Ortec Alpha-Esemble-8 fitted with Silicon Charged Particle Radiation Detectors. The Ortec High Purity Germanium Gamma Ray detector was used for detection of Ra decay. Efficiency and energy calibrations for the two detectors were determined using a calibration source containing gamma/alpha emitting radionuclides with certified activities traceable to the National Institute of Standards and

Technology (NIST). Selection of depths for plutonium analysis, was based on preliminary ^{210}Pb dating results, eleven samples were selected for analysis from 10.25 cm to 30 cm. An extended methodology for plutonium analysis is outlined in Appendix D. Plutonium activities were measured in the VEGA 1MV accelerator system at ANSTO, following the techniques outlined by Hotchkis et al. (2019). Various intervals from WB86 were analysed for radiocarbon ages, ostracod samples were analysed using the Small Tandem for Applied Research Accelerator (STAR) and the Australian National Tandem Research Accelerator (ANTARES).

The results from ^{210}Pb analysis were used as to model sediment ages using the constant initial concentration (CIC) and constant rate of supply (CRS) models as outlined by Appleby and Oldfield (1978), for which dry bulk densities were determined using the protocols outlined in Appendix E. The combined radiocarbon and lead ages were then used to develop a composite age-depth model using the package Bacon in 'R' (Blaauw & Christen 2011).

3.3 SEM Imagery

Ostracods from a WB15 sample at 9.25 cm were imaged using the FEI Quanta 450 FEG Scanning Electron Microscope at the Adelaide Microscopy facility. The ostracods were mounted and carbon coated for backscatter electron (BSE), secondary electron (SE) and energy dispersive x-ray spectroscopy (EDS). Imagery was collected using a spot size 4 and 15k V beam voltage. Results were acquired using an Oxford Instruments Ultim Max 170 mm SDD EDS Detector with Aztec software.

3.4 Stable Isotopes

3.4.1 OSTRACOD SAMPLE PREPARATION

Ostracods were prepared for Isotope Ratio Mass Spectrometry (IRMS) by wet sieving each sediment sample at 250 μm and 125 μm, using deionised (DI) water. Each size fraction was retained for analysis, with the coarse fraction used for Ostracod analysis. Samples from 0-10 cm, 27.5-33.5 cm and 36.5-39.0 cm were freeze dried and manually cleaned by suspension in ethanol and removal of organic matter (OM) and clay using a needle, brush and tweezers. The samples from 10.0-27.5 cm and 33.5-36.0 cm had been oven dried for the above chronological analysis. Disaggregation of these samples was achieved by soaking in a 5% sodium hexametaphosphate solution for 24 to 48 hours prior to sieving at 250 μm as above. These samples were then placed in 18 % H_2O_2 solution, buffered to a pH of 8 with 0.5 M NaOH, and reacted at 50 ºC for 4 to 6 hours to remove OM that had adhered to the ostracod shells as a result of the drying process. Once complete, the samples were rinsed with DI water and placed in 50 ml centrifuge tubes and stored at 4 ºC, before ostracods were manually removed as above.

3.4.2 BULK INORGANIC CARBONATE PREPARATION

Fine carbonate samples were prepared for oxygen and carbon isotope analysis by retaining the portion of sediment <125 μm. As above, some samples were sieved from wet sediment samples others from material which had previously been dried. Dried samples were disaggregated prior to sieving, using the methods described above. All samples were rinsed with DI water and centrifuged four times to remove any sodium hexametaphosphate. Carbonate fractions were also treated with the pH buffered H_2O_2 solution described above, for 4 to 5 hours at 50 ºC, left in solution overnight, rinsed, and

treated for a further 4 to 5 hours at 50 ºC before being rinsed again, freeze dried and weighed for IRMS analysis.

3.2.3 IRMS ANALYSES

Analyses were performed using a Nu Horizon Isotopic Ratio Mass Spectrometry (IRMS) coupled via continuous flow to a Nu Gas Bench preparatory device. BIC Samples were reacted in borosilicate vials with 105% phosphoric acid at room temperature (20 ºC) and 70 ºC for one to two hours, while the Ostracods were only reacted at 70ºC. Ostracod and BIC samples were analysed against carbonate standards which were measured to 0.2 to 1.1mg to account for sample size variation. Laboratory Standards used were UAC-1 ($\delta^{18}O$ = -18.4 ‰, $\delta^{13}C$ = -15.0 ‰), NCM ($\delta^{18}O$ = -1.92, $\delta^{13}C$ = 2.09) and ANU-P3 ($\delta^{18}O$ = -0.32 ‰, $\delta^{13}C$ = + 2.2 ‰). The standards were arranged so there were six standards at the start of each run and an additional six at the end, including one blank (an empty vial). There were also two standards for every ten samples, resulting in 28 standards for every 72 samples.

4.0 RESULTS

4.1 CHRONOLOGY

The ^{210}Pb chronology results (Table one) show total, supported and the resulting unsupported ^{210}Pb activity decrease down-core, consistent with the radioactive decay of ^{210}Pb, though there are some points that deviate from the trend (Figure 3a and 3b). When compared to the graph of accumulation rate with depth (Figure 3c) these deviations coincide with variations in accumulation rate. The CIC and CRS modelled ages calculate similar ages until 20 cm, where the CRS model predicts an age of 118 years at the maximum sample depth, with an accumulation rate of approximately 0.3

cm/year (Figure 3d). The CIC model suggests a maximum age of only 89 years and an accumulation rate of approximately 0.4 cm/year.

The results of the plutonium dating (Table 2) show a peak in the total Pu around 20.5 cm, which also corresponds with an increase in the $^{240/239}$Pu ratio (Figure 3e). This indicates that approximately 20.5 cm in the core should represent sediment deposited after the 1963 nuclear bomb tests in the Northern Hemisphere (Bollhöfer et al., 1994). Applying the CIC and CRS ages to the depths at which total Pu was measured, allows comparison between the two techniques and validation of the two models. On this basis, the 1963 nuclear testing aligns with the initial rise in the Pu concentration based on the CRS age model (Figure 3f) yet not with that derived using the CIC model.

The radiocarbon age/depth model (Figure 4) indicates that the accumulation of sediment in West Basin has been constant throughout the Holocene, predicting a 0.1 cm/year sedimentation rate. This is at odds with the 0.3 to 0.4 cm/year predicted by the lead chronology.

Table 1. Results from lead-210 dating. Dry bulk density was calculated following the protocols outlined in Appendix D. Total ^{210}Pb was calculated from alpha decay of Po, and Supported ^{210}Pb from gamma decay of Ra. This was used to calculate the Unsupported ^{210}Pb (Unsupported = Total – Supported). The resulting CIC and CRS ages were then calculated using these results.

Sample Depth (cm)	Dry Bulk Density (c/cm^3)	Total ^{210}Pb (Bq/kg)	Supported ^{210}Pb (Bq/kg)	Unsupported ^{210}Pb (Bq/kg)	Calculated CIC ages (years)	Calculated CRS ages (years)
0.25 - 0.75	0.03	133 ± 6	28 ± 3	104 ± 6	0.1 ± 0.1	0.1 ± 1.4
2.00 - 2.25	0.13	141± 7	39 ± 4	102 ± 8	1.9 ± 0.2	2.0 ± 2.4
3.0 - 3.25	0.13	69 ± 3	8 ± 1	62 ± 3	3.6 ± 0.4	3.6 ± 2.4
4.5 - 4.75	0.13	50 ± 2	6 ± 1	43 ± 2	6.3 ± 0.7	5.2 ± 2.5
5.25 - 5.5	0.13	81 ± 4	6 ± 1	75 ± 4	8 ± 1	6 ± 3
8.5 - 8.75	0.13	71 ± 3	12 ± 1	60 ± 4	13 ± 1	11 ± 3
10.75 - 11.0	0.13	106 ± 5	12 ± 1	94 ± 5	17 ± 2	16 ± 3
13.0 - 13.25	0.13	53 ± 2	9 ± 1	45 ± 2	21 ± 2	21 ± 3
15.0 - 15.25	0.13	72 ± 4	9 ± 1	64 ± 4	25 ± 3	24 ± 3
15.25 - 15.5	0.17	52 ± 3	14 ± 2	39 ± 3	25 ± 3	25 ± 3
19.75 - 20.0	0.17	70 ± 4	13 ± 1	57 ± 4	36 ± 4	38 ± 4
22.0 - 22.5	0.21	57 ± 2	13 ± 1	46 ± 3	42 ± 5	51 ± 5
25.0 - 25.5	0.21	28 ± 1	13 ± 1	15 ± 2	51 ± 6	65 ± 6
27.0 - 27.5	0.21	24 ± 1	13 ± 1	11 ± 2	56 ± 6	72 ± 6
33.5 - 34.0	0.30	20 ± 1	14 ± 1	7 ± 2	79 ± 9	99 ± 10
36.0 - 36.5	0.30	20 ± 1	14 ± 1	7 ± 2	89 ± 10	118 ± 13

Table 2. Results of Pu dating. Sample depths were chosen based on preliminary 210Pb results. The concentrations of the two Pu isotopes of interest and total Pu were measured via AMS.

Sample Depth (cm)	^{239}Pu Concentration (pg/g)	^{240}Pu Concentration (pg/g)	Total Pu Concentration (pg/g)	$^{240/239}$Pu Atomic Ratio
10.25	0.0109 ± 0.0007	1.66E-03 ± 1.17E-04	0.0125 ± 0.0007	0.153 ± 0.018
14.25	0.0149 ± 0.0005	2.08E-03 ± 6.96E-05	0.0170 ± 0.0005	0.140 ± 0.006
16.25	0.0310 ± 0.0009	4.04E-03 ± 1.37E-04	0.0350 ± 0.0009	0.131 ± 0.005
18.25	0.1586 ± 0.0037	1.22E-02 ± 2.93E-04	0.1708 ± 0.0037	0.077 ± 0.002
20.5	0.1885 ± 0.0047	3.10E-02 ± 7.69E-04	0.2196 ± 0.0048	0.165 ± 0.004
22.5	0.1251 ± 0.0036	1.52E-02 ± 4.66E-04	0.1403 ± 0.0036	0.122 ± 0.003
24.5	0.0026 ± 0.0002	3.27E-04 ± 2.83E-05	0.0029 ± 0.0002	0.128 ± 0.011
25.5	0.0028 ± 0.0002	4.53E-04 ± 3.21E-05	0.0033 ± 0.0002	0.160 ± 0.011
26.5	0.0021 ± 0.0002	4.05E-04 ± 3.60E-05	0.0025 ± 0.0002	0.192 ± 0.022
27.5	0.0003 ± 0.0000	3.31E-05 ± 8.22E-06	0.0004 ± 0.0000	0.101 ± 0.027
30	0.0001 ± 0.0000	4.57E-06 ± 8.51E-06	0.0001 ± 0.0000	0.036 ± 0.041

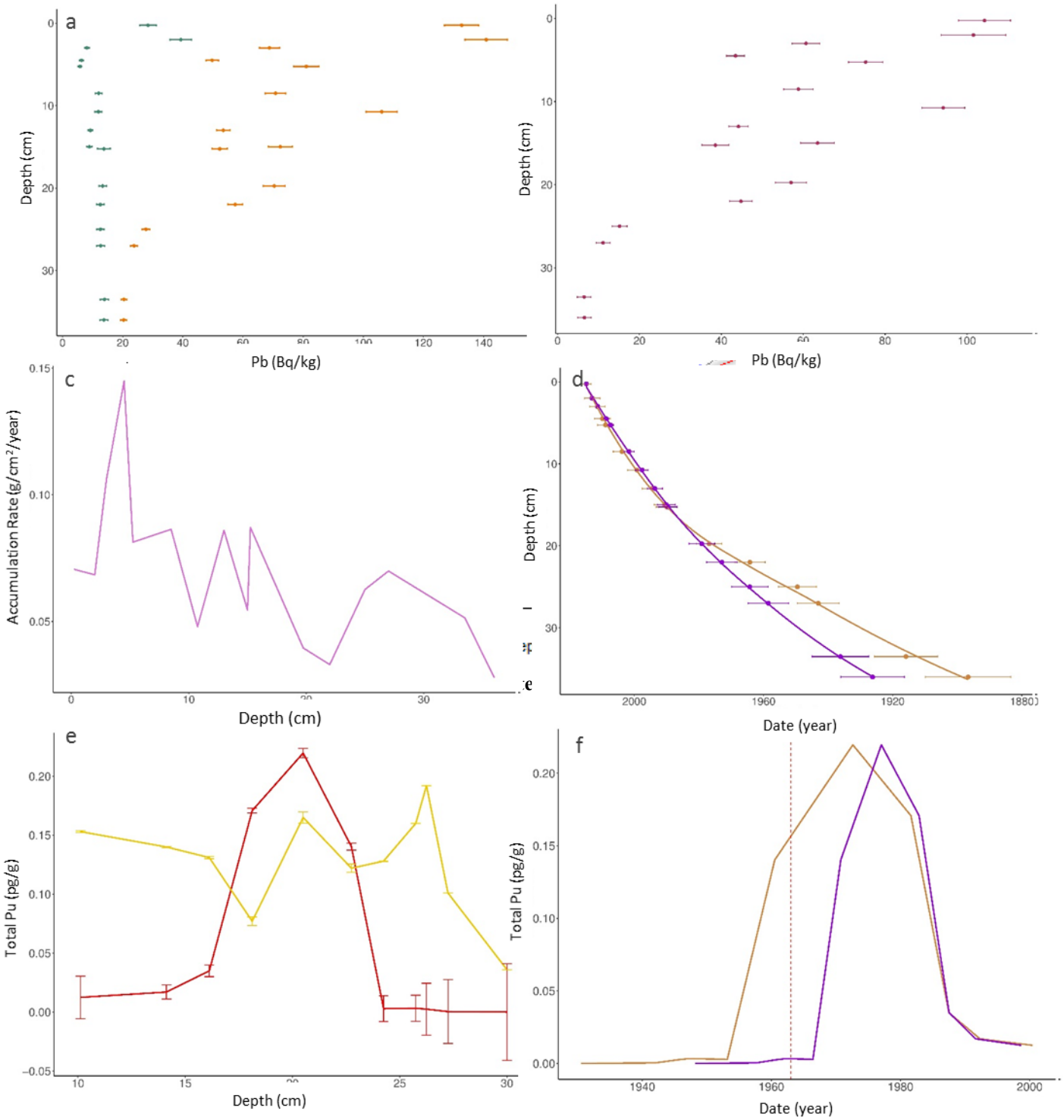

Figure 3. Results from 210Pb and Pu chronology a) Total (orange) and supported (green) lead activities (Bq/kg) against depth (cm) b) Unsupported lead activity calculated as 'unsupported = total - supported' against depth (cm) c) Accumulation rate vs. depth (cm) d) Constant initial concentration (CIC) (purple) and constant rate of supply (CRS) (gold) age models against depth (cm). e) Total Pu (red) and 239/240Pu ratio (yellow) against depth (cm). f) CRS (gold) and CIC (purple) model ages against total Pu. Red dashed line shows where 1963 lies for reference.

4.2 SEM Imagery

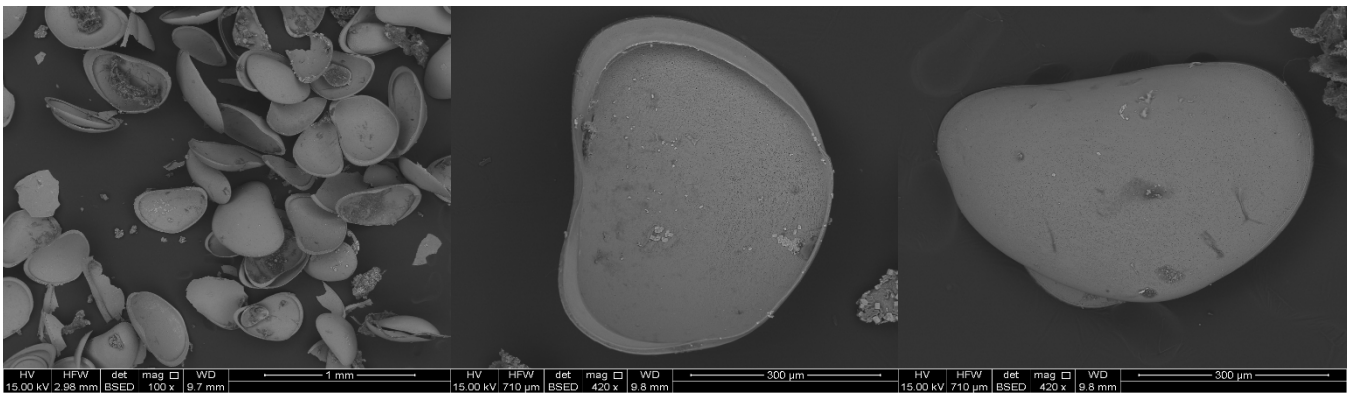

Figure 5. SEM images of Ostracods from 9.25cm. Left: SEM image of ostracods from the sample at 100x magnification. This image shows the shells are largely intact, do not appear be contaminated with re-precipitated calcite and all belong to one species. Middle: SEM image at 420x magnification of inside one shell to show internal structure and presence of contaminants. Right: SEM image at 420x magnification of outside of same shell to show external texture and presence of contaminants.

The results of the SEM imagery (Figure 5) show that the majority of Ostracod shells in this sample are all of the same species and maturity. These results also show the shells are largely undamaged and the sample contains minimal contamination. The images in Figure 5 have been used to identify the species as *Diacypris Compacta* as this species has been shown to be present by (Gell et al., 1994).

EDS analysis was undertaken on the sample in Figure 5, and is presented in Appendix F. This allows for the composition of the contaminants seen in Figure 5 to be determined. From this, the contaminants were found to be largely consist of Na. Cl, Al, Si, Mg, Fe and S. There were also some sites that contain small C and O signals, outside of that from the Ostracod shell.

4.3 Carbonate Analyses

Both the BIC isotopic analyses show positive correlation between the carbon and oxygen values, with the carbon values showing a more positive correlation and less

scatter (Figures 6a and 6b). Scatter in Figure 6a decreases with increasing values. The Ostracod carbon values, when compared to the average of the BIC data, show no relationship, exhibiting heavy scatter (Figure 6c). The correlation between the Ostracod oxygen and averaged BIC oxygen (Figure 6d), show agreement, but are still heavily scattered.

Figure 7, demonstrates a positive relationship between each combination of oxygen to carbon analyses. The cold BIC data (Figure 7a) exhibits heavier scatter than the hot BIC (Figure 7b). When the average of these results is taken (Figure 7c), the scatter increases and the cold BIC signal dominates. There is a less positive trend and increased scatter when the Ostracod data is plotted together (Figure 7d).

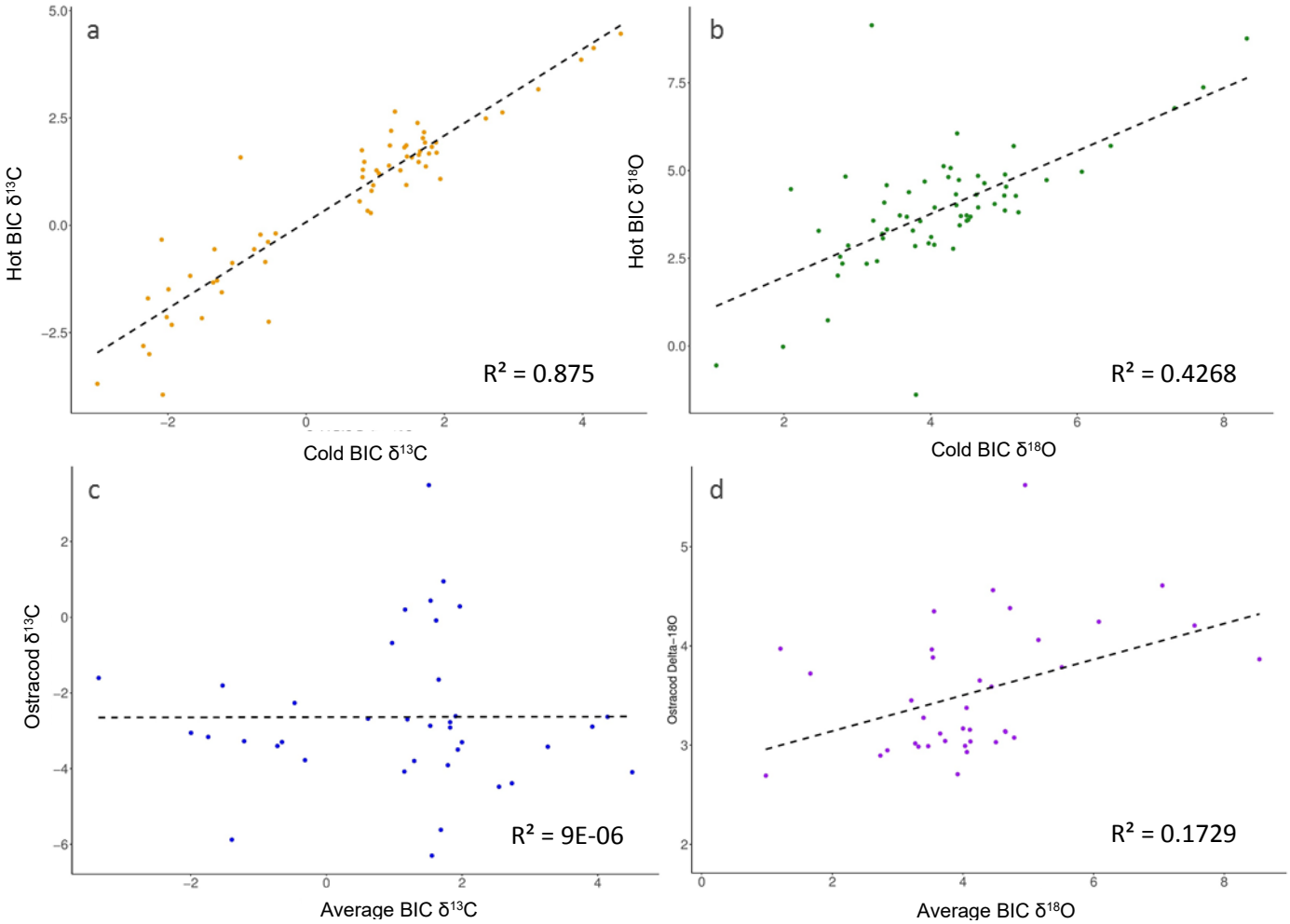

Figure 6. Plots of Carbon and Oxygen isotopic data correlations. a) Plot of hot BIC carbon isotopes against cold BIC carbon isotopes. b) Plot of Hot BIC oxygen isotopes against cold BIC oxygen isotopes. c) Plot of Ostracod carbon isotopes against averaged BIC carbon isotopes. d) Plot of Ostracod oxygen isotopes against averaged BIC oxygen isotopes.

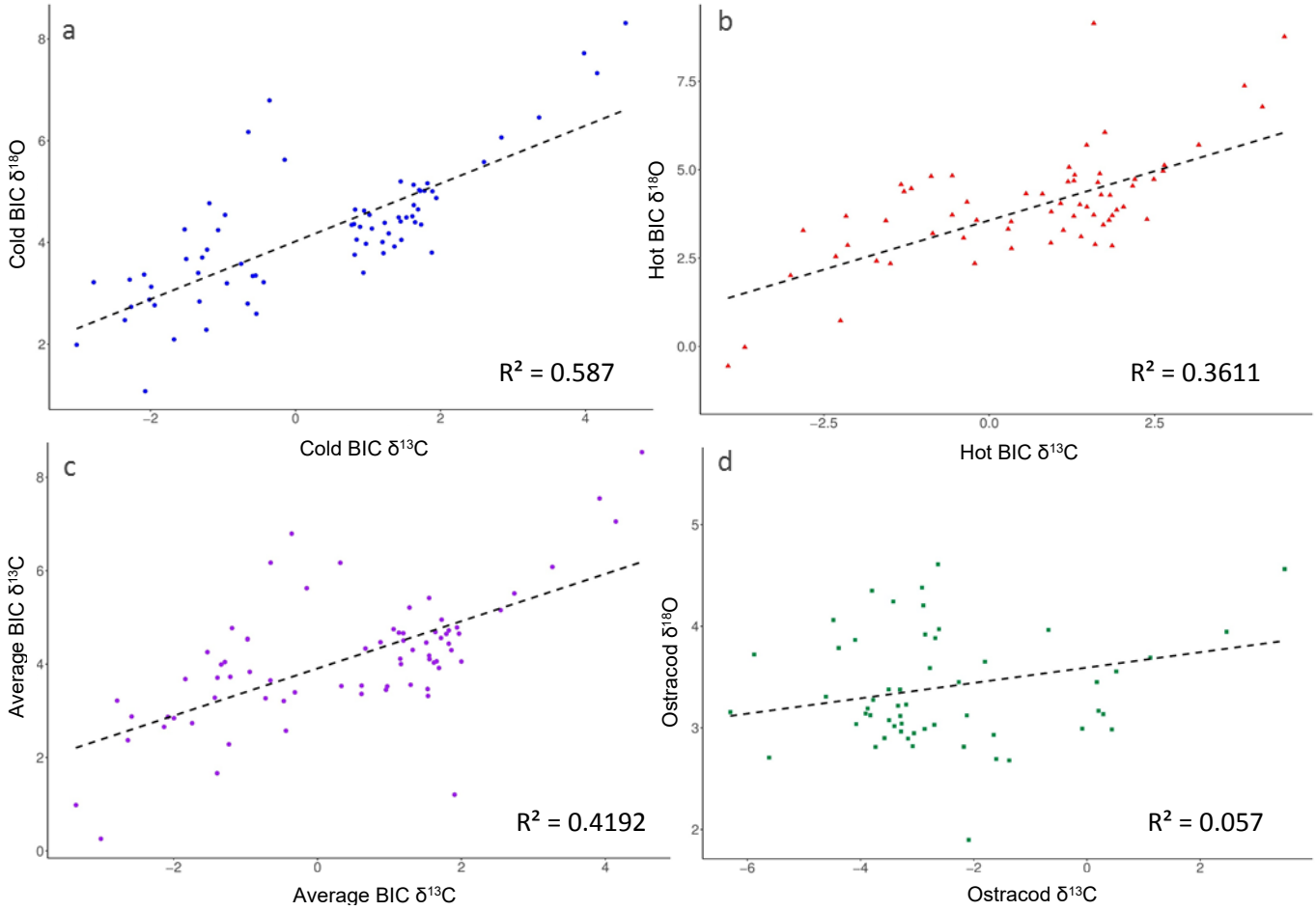

Figure 7. Plots of correlation between oxygen and carbon isotope values for a) cold BIC b) hot BIC c) averaged BIC d) Ostracod calcite.

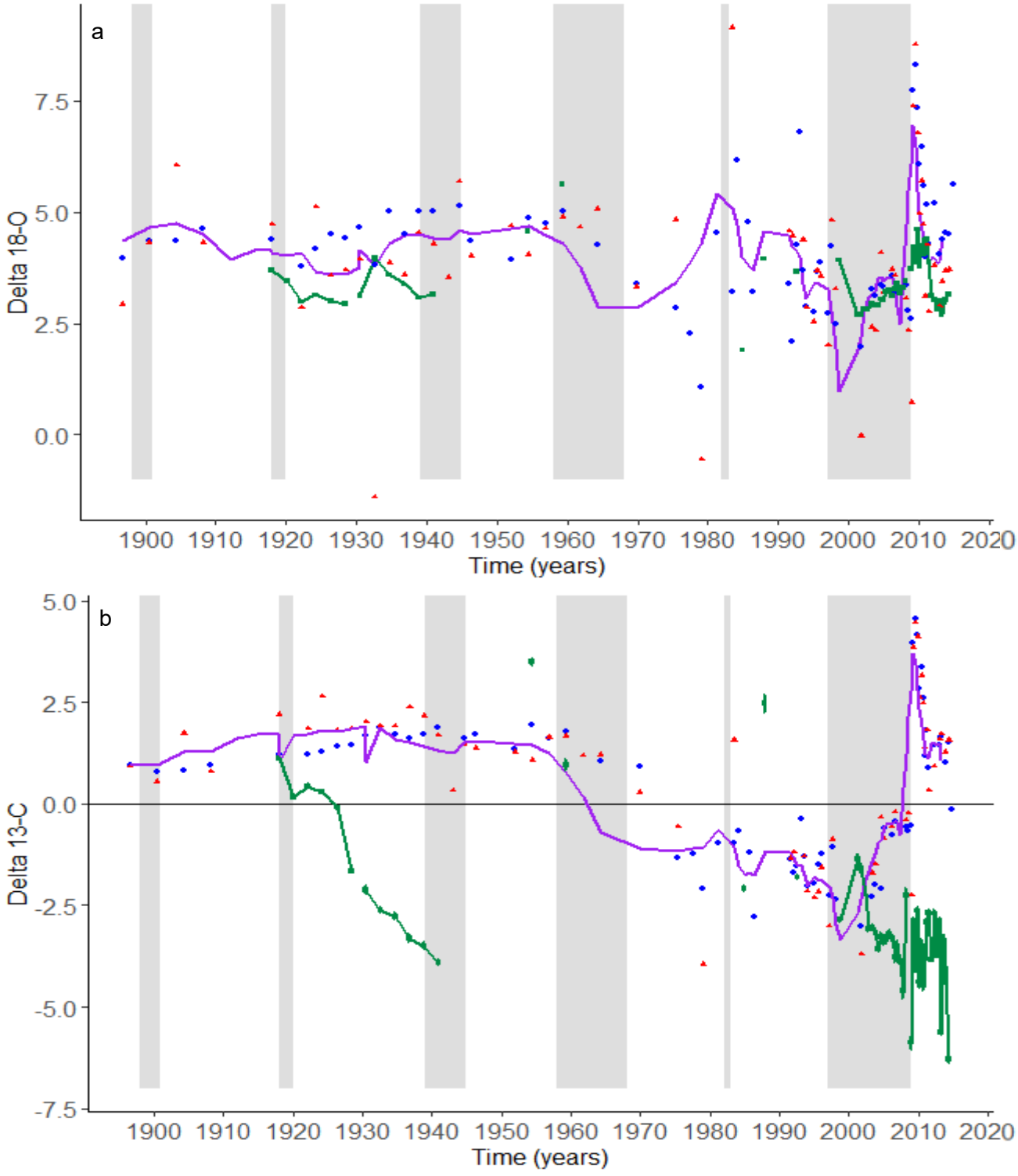

Figure 8. Graphs of results of isotopic analyses against time, calculated using the CRS age model. Top) Results of oxygen analyses of Ostracods (green), cold BIC (blue), hot BIC (red) and average BIC (purple) against time (years). Bottom) Results of carbon analyses of Ostracods (green), cold BIC (blue), hot BIC (red), and average BIC (purple) against time (years). Grey zones represent major Australian drought periods. Left to right; The Federation Drought, 1918-1920 drought, the WWII Drought, 1958-1968 drought, 1982 drought, and the Millennium Drought.

Figure 8a shows good agreement between both proxies. These proxies depict similar trends in both the oxygen and carbon isotopic results. The purple line, which represents a five year running average of the BIC data, shows good agreement with the data points of both the hot and cold BIC runs, and smooths the trend, particularly in areas where the hot and cold values have large discrepancies.

The majority of the oxygen results for both proxies lie between 2.5 ‰ and 5.0 ‰, with peaks often occurring during or after major drought periods. In both proxies, the younger data is more concentrated and therefore more variable, but shows a clear increasing trend during and after the Millennium Drought. The carbon isotopes are more variable and lighter than oxygen. This data also has a less defined relationship to drought occurrence, though the overall trend somewhat mimics that of the oxygen. Carbon values exhibit less scatter for the two BIC runs, resulting in better agreement with the 5 year average. The Ostracod values are almost consistently lighter than that of the BIC which shows a more pronounced trend from 1920 to 1940. The Ostracod data is also more variable at the time of the Millennium Drought, than the corresponding BIC values.

Figure 8. Timeseries Oxygen data with the five year moving average BIC (Purple). Green line is the Ostracod data, which was unable to be averaged due to the large temporal gaps in the data. Grey zones represent major Australian drought periods. Left to right; The Federation Drought, 1918-1920 drought, the WWII Drought, 1958-1968 drought, 1982 drought, and the Millennium Drought

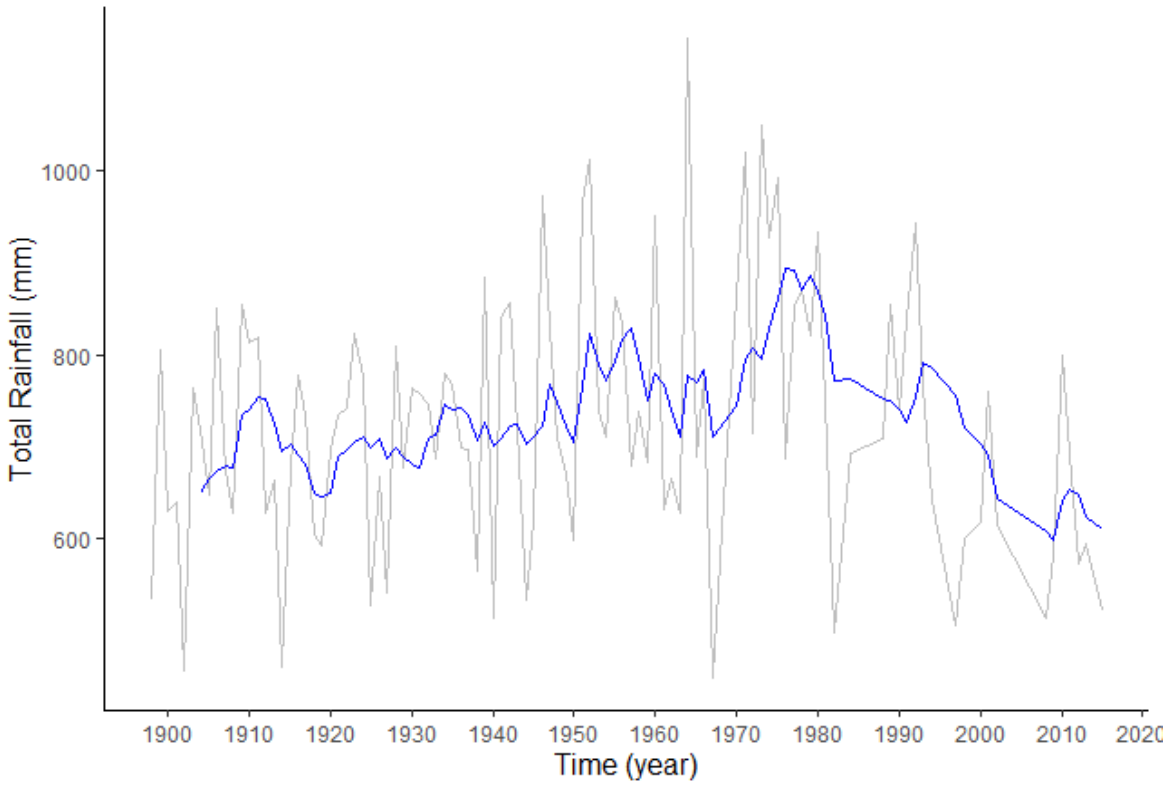

Figure 9. Total annual (grey) and five year average (blue) rainfall (mm) at Colac station against time (years).

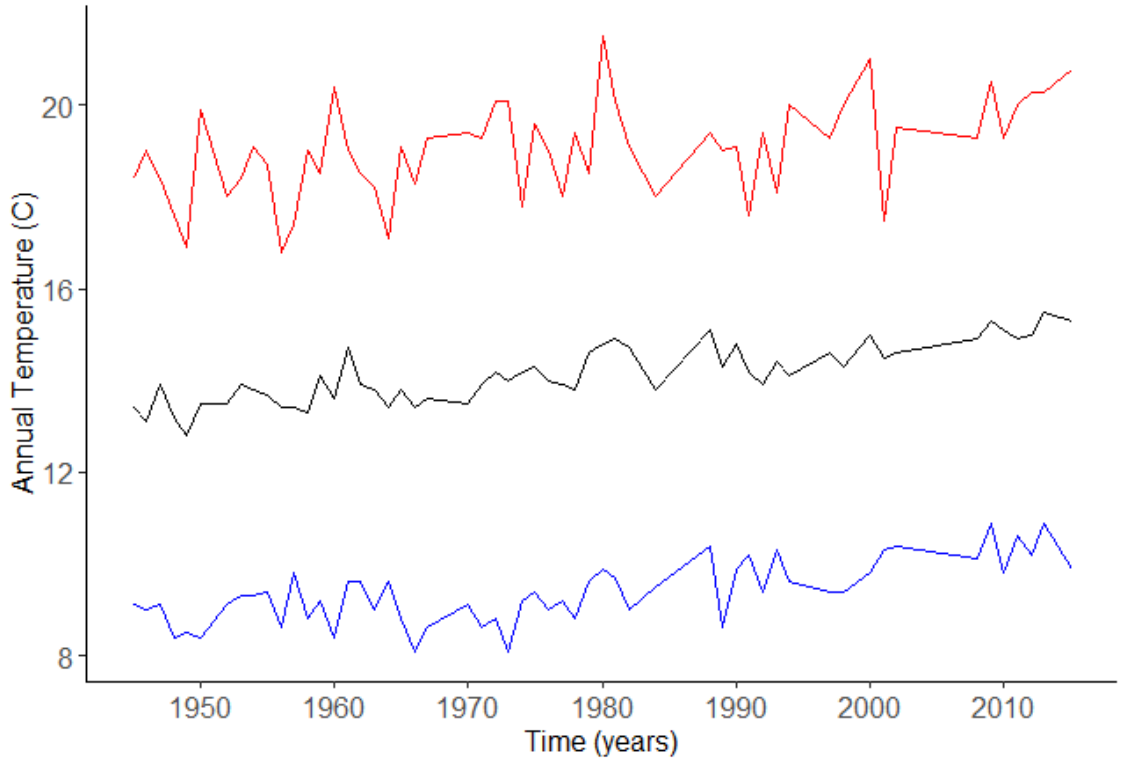

Figure 10. Timeseries of mean temperatures (C) against time (years). Mean annual temperature (black), mean summer temperature (red) and mean winter temperature (blue) from Colac station.

The five year averaged oxygen trend and Ostracod data in Figure 9 allows for comparison between instrumental rainfall (Figure 10) and temperature (Figure 11) data from Colac station. The purple averaged line, mainly mirrors the five year average rainfall trend. There is a peak, however, in the $\delta^{18}O$ values from 1900 to approximately 1910 that correlates to an overall trend of increased rainfall, though the annual data (grey) suggests there are two significant low years during this time.

The period following this, which includes the 1918 to 1920 drought period, is mirrored by a peak in the BIC, and where the Ostracod data is present, this proxy picks up the decrease post peak. Disagreement is evident between the BIC and Ostracod data between 1930 and 1940, though there is a small peak in the BIC which appears slightly earlier. The Ostracod $\delta^{18}O$ may be responding to a small decrease in the rainfall that

occurs after 1930. Once the temperature record starts, there is further agreement between this trend and those of the rainfall and $\delta^{18}O$ values. The extensive drought period that took place from 1958 to 1968 corresponds to large variation in the annual rainfall, and increased temperatures over this period (Figure 11). Following this period, there is a large increase in rainfall in both the annual and five year average, during which $\delta^{18}O$ values are the second lowest in this record. A sharp peak in $\delta^{18}O$ values is seen at the 1980 mark, which correlates with a large trough in annual rainfall and peak in temperature.

The Millennium Drought exhibits the most variable $\delta^{18}O$ signal, though has the most agreement with the annual rainfall data, rather than the five year average. This period also corresponds to increased temperatures, particularly a period of consistently warmer temperatures.

5.0 Discussion

Validating paleoclimate proxies is an important step towards obtaining robust records of past climate variability (Dean et al., 2015). Ideally paleoclimate records should have demonstrated validity in time, however there are several barriers that prevent this in the majority of lake sediment archives. These barriers include the impact of anthropogenic disturbance on lake sediments (Gouramanis et al., 2010), as well as the challenges of obtaining highly resolved and precisely dated sediments which span the instrumental period (Barr et al., 2014; Dean et al., 2015). In this context, the sediments of West Basin Lake are rare, since they rapidly accumulated over the last century, and facilitate the development of high quality radiogenic age model for that period (Gell et al., 1994; Last & De Deckker, 1990; Lockier, 2015; Prodan, 2014). This study is one of the first in the region to conduct such a high resolution reconstruction of paleohydrology.

5.1 Chronology

To determine if the proxies examined in this study can be validated, the δ18O results in Figure 9 have been examined against major droughts, and compared to yearly annual and five year average rainfall data from Colac station (Figures 10 and 11). Both proxy systems show good agreement with drought periods and decreasing/increasing rainfall.

In order to make an assessment of the validity of the isotopic data collected in this study, the accuracy of the high resolution chronology must be determined.
The two age models calculated from the results of the ^{210}Pb chronology show remarkable agreement until approximately 20 cm depth. Beyond this depth, the CRS model predicts older ages than the CIC model. This disagreement between the two models stems from differences in assumptions made by each (Appleby & Oldfield, 1978). Thus, a determination on which is more accurate is made by comparison of these models to the Pu analyses. Pu as a tracer, is a relatively recent advancement in dating methodology in the Southern Hemisphere (Sanders et al., 2016). This advancement is largely due to recent improvements in the detection rate for the small amounts of Pu retained in sediments (Sanders et al., 2016). The Pu peak and isotopic ratios in Figure 3e are a signature of the Northern Hemisphere bomb testing, and therefore the peak can be reliably dated to 1963 (Bollhöfer et al., 1994). An ideal Pu curve should display only background levels of Pu both pre and post bomb peak, which is almost perfectly displayed in the profile in Figure 3d. When this profile is combined with the results of the ^{210}Pb chronology, the initial rise in Pu correlates well with the initial rise in the CRS model. The peaks of both models predict dates younger than the suggested Pu horizon, which indicates that further Pu and ^{210}Pb analysis may improve the accuracy of this age

model. However, given the CRS model peak has the closest overlap with the Pu results, this model is the more accurate of the two. As a result, this age/depth profile has been used to assign dates to the results of the isotopic analysis in this study with a good degree of confidence.

One of the barriers to analysing proxy data at such high resolution, further back in the geological record is the ability to date sediments accurately. The radiocarbon chronology in Figure 4 displays a smooth down-core chronology, predicting approximately 100cm of sediment every 1000 years. This works out to be 0.1 cm/year, at odds with the ^{210}Pb chronology, which predicts a much higher sediment accumulation rate of approximately 0.5 cm/year. Radiocarbon and lead dating often disagree as there is an issue with the input of 'old' carbon from other sources which skews ages towards older dates (Barr et al., 2014; Blaauw et al., 2011). To overcome this, the lead chronology can be used to calculate the offset that results from 'old carbon' input, though there is still some uncertainty (Barr et al., 2014; Blaauw et al., 2011). Regardless of this, radiocarbon in conjunction with lead dating remains the best method of age/depth modelling for sediments.

5.2 Proxy Data Analysis

The resulting time series data in Figure 8 and 9 correlates well with the rainfall data in Figure 10. Values of δ^{18}O often display increasing trends and peaks associated with periods of drought or low average rainfall. This response of δ^{18}O to changes in P:E is not displayed in the results as a permanent increase/decrease in values. The system will respond to a sudden change in P:E with the corresponding increase or decrease, and will then move towards a new base state as modelled by (Jones, Leng, Roberts, Türkeş, &

Moyeed, 2005). This model, which was based on observed responses to evaporation change in Lake Nar, was simplified in order to investigate the effect on a lake isotope balance of an abrupt shift in evaporation without a corresponding change in temperature (Jones et al., 2005). Such a shift would not occur in isolation in nature, and as such the response of the isotope system does not display the ideal change observed in the model (Jones et al., 2005). This is however, an indicator as to the trends that are likely to be seen in the results of this study. An example of this shift can be seen in Figure 8. This signal is present, to an extent, throughout the record, though is often masked by other changes such as temperature, which also affects the isotopic budget of the lake (Dean et al., 2015; Jones et al., 2005).

Another important consideration for evaluating the response of proxies to climate is the fractionation factors between the proxy and the lake system. Ostracods vary in their vital effects from species to species, which results in varying degrees of positive shifts away from the isotopic value of the lake water (Decrouy et al., 2011; Kalm & Sohar, 2010). These effects however, are likely consistent through time, and therefore if a single species is used, these vital effects should all display the same enrichment from lake values through the record (Kalm & Sohar, 2010). The carbonate content of West Basin Lake was studied in detail by (Last & De Deckker, 1990). Their analysis determined that fractions of carbonate species in the sediment through time. BIC content found to be largely calcite and dolomite, with lesser amounts of magnesite and hydromagnesite (Last & De Deckker, 1990). As different carbonate species have different fractionation factors, ideally these species would be analysed separately (Al-Aasm, Taylor, & South, 1990).

The small amount of error that could result from this difference was assessed, in part, by analysing BIC at room temperature (20 °C) and again at 70 °C. For the most part, this produced negligible differences in isotope values, and the average of both runs was used for comparison against instrumental data. The carbon isotopic values of these two runs have an R^2 value of 0.875 when plotted together, indicating that analysing the samples at two different temperatures may not be necessary for investigations of carbon isotopes. The agreement between the oxygen results for the two BIC runs had mid-range R^2 (0.468) which is still good agreement considering the low carbon concentration of the samples. This method would benefit from x-ray diffraction analysis in future, to determine which carbonate minerals are present for those samples where a large difference is found. The effects of $\delta^{18}O$ enrichment in Ostracod calcite were deemed consistent due to SEM imagery (Figure 5) of a sample, which confirms there is only one species present. The EDS analysis of the same sample (Appendix F) show that these contaminants are largely made up of elements such as Na and Cl which would be a legacy of the saline conditions within the lake. There was also commonly Fe, Mg, Al and Si which indicate the presence of clays. Salt and clay contamination does not affect the results of IRMS analysis. Small amounts of C and O outside of the shells themselves indicate organic or BIC contamination. However, the relatively smooth trends between samples when plotted, would indicate that the presence of other sources of C and O have little effect on the overall results. The $\delta^{18}O$ values determined from BIC analysis, though more isotopically enriched, often mirrored those of the Ostracod calcite. Therefore, these results are also deemed consistent based on the assessments of the Ostracod reliability.

In addition to fractionation, it also important to assess the source of carbonates to determine if they can be used to reliably infer changes in lake chemistry and therefore P:E. In the case of Ostracods, they are almost certainly endogenic, as the organisms lives within the lake water and samples lake water to build their calcite shells (Bright, Kaufman, Forester, & Dean, 2006). Last and De Deckker (1990) determined that the BIC within West Basin Lake had very little detrital input. As a result, both proxies can be determined to reliably reflect lake water chemistry and therefore P:E changes. Interpretation of the $\delta^{13}C$ results add to the $\delta^{18}O$ data, though carbon isotopes in lakes are not often used as a primary climate proxy due to the large variety of controls on $\delta^{13}C$ of lakes (Bright et al., 2006). These controls include: methanogenesis, biological productivity, photosynthesis, and pH (Bright et al., 2006). When there is interpretation of trends in carbonate $\delta^{13}C$, they are most often described as indicative of changes in the carbon cycle within the lake (Holmes et al., 1997) or as indicative of closed basin lakes, if the R^2 is near 0.7 (Bright et al., 2006).

The R^2 values for most runs in this study are relatively low, though they all exhibit positive trends. The highest R^2 value for the oxygen and carbon relationships was 0.587, which is lower than the suggested value for a closed basin (Bright et al., 2006). If West Basin Lake was receiving water from a source other than precipitation, it would not be able to reliably record changes in P:E. However, much of the previous study in the region has determined that the lake is largely closed, receiving very little groundwater input (Last & De Deckker, 1990). Therefore, it is likely that these R^2 values are affected by the low carbonate concentration of the samples.

Low carbonate content in the BIC samples lead to low detection and high reported error in the IRMS analyses. The low carbonate content could be a result of several factors, including treatment, sampling or varying carbonate production. The treatment used to remove organic matter, despite the solution being buffered to a pH of 8, has been shown to break down to acidic ions at a temperature of 75 ºC which would o result in loss of carbonate (Falster, Delean, & Tyler, 2018). While previous work by Falster et al (2018) showed that this did not occur at the conditions used (which have been replicated here), it is possible that this may have occurred if the temperature of treatment exceeded 50 ºC, however this explanation seems unlikely. Low inorganic carbonate is, in all probability, a result of the conditions within the lake itself. The sedimentation rates determined from the lead chronology are fast for a lake, which may result in carbonate dilution. Some samples were affected more than others, with some not containing detectable levels of BIC. Such changes in carbonate concentration could be a result of increased sediment influx, as well as variation in the precipitation of carbonate with time. This could be due to factors such as organic productivity, pH and temperature, among others (Last & De Deckker, 1990).

5.3 Comparison to Other Studies and Future Research

The previous studies in West Basin Lake (Gell et al., 1994; Last & De Deckker, 1990; Lockier, 2015; Prodan, 2014) have all been conducted on much coarser and longer timescales, limiting the ability to draw comparisons between this study and the previous. The same is true for many of the regional studies (Gouramanis et al., 2010; Wilkins et al., 2013). The studies that have been conducted in this region all show increasingly dry hydrological conditions over the period since European Settlement (Barr et al., 2014; Gell et al., 1994; Tibby, Tyler, & Barr, 2018; Wilkins et al., 2013).

This trend is not apparent here due to the limited time frame of instrumental data upon which to compare the proxy record.

Future work in this field would benefit from improved radiocarbon and lead chronology, in order to use the findings of studies such as this, to extrapolate further through the geological record. This study, and similar studies (Dean et al., 2015; Li, Ku, Stott, & Anderson, 1997; Ricketts & Anderson, 1998) have shown that it is possible to conduct high-resolution $\delta^{18}O$ profiles that can reliably reflect drought periods, though further studies conducted on multiple proxies would create a broader scope for this kind of research. Studies such as these can be used to quantify the changes in P:E throughout the geological record. Doing so would add greatly to our understanding of the drought record in Australia, and allow for accurate assessments of the impacts of human activity and climate change on regional hydrology.

6.0 CONCLUSIONS

This study set out to assess the validity of Ostracod and BIC in lake sediments as proxies for P:E change. A high-resolution reconstruction of oxygen and carbon isotope variability from West Basin Lake was successfully created and good agreement between the isotopic profile and the instrumental record of precipitation was found. From the comparisons made between the instrumental climate data, it was determined that Ostracod calcite and BIC are reliable records of paleohydrology and are able to record fine changes in the isotopic composition of lake water, which makes them excellent for high resolution paleoclimate studies. Both carbonates often exhibit the same trends and have very similar isotopic values with this agreement adding confidence to both as paleohydrological proxies. Ostracod calcite records a higher degree of precision in

isotopic values than that of BIC. However, as demonstrated, the BIC is able to produce a much more consistent isotopic record. These results show that high resolution reconstructions are possible for the instrumental record. Such findings mean that with further research, proxy system models that rely on modern understandings of proxy systems can be improved and used for higher resolution studies. Such studies may be able to reconstruct drought history in Australia past the time frame of instrumental data, which allow for modern droughts to be compared against those of the past with increased accuracy. Such comparisons would allow for the understanding of the effects of human induced climate change on weather systems, such as ENSO and IOD which govern Australia's rainfall.

7.0 ACKNOWLEDGMENTS

Thanks are given firstly to Jonathan Tyler for his guidance and assistance as primary supervisor throughout this project. I would also like to thank Cameron Barr for providing additional support as secondary supervisor.
The author would also like to thank AINSE for their scholarship funding for this project.
Thanks also to Atun Zawadzki, David Child, Sabika Maizma and Jay Chellappa as well as the rest of their teams at ANSTO for their work in creating the ^{210}Pb and Pu chronology.
Special thanks to Robert Klaebe, Tony Hall and Kristine Nielson for their assistance with IRMS analyses.
I would also like to thank Haidee Cadd for lab instruction and assistance.
Lastly, thanks to Ken Neubauer from Adelaide Microscopy for his work in SEM and EDS imaging.

8.0 REFERENCES

AL-AASM, I. S., TAYLOR, B. E., & SOUTH, B. (1990). Stable isotope analysis of multiple carbonate samples using selective acid extraction. *Chemical Geology: Isotope Geoscience Section, 80*(2), 119-125. doi:10.1016/0168-9622(90)90020-D

APPLEBY, P., & OLDFIELD, F. (1978). The calculation of lead-210 dates assuming a constant rate of supply of unsupported lead-210 to the sediment. *Catena, 5*, 1-8.

AUSTRALIAN BUREAU OF STATISTICS. (2012). Drought in Australia. Retrieved from https://www.abs.gov.au/AUSSTATS/abs@.nsf/lookup/1301.0Feature%20Article151988

BARR, C., TIBBY, J., GELL, P., TYLER, J., ZAWADZKI, A., & JACOBSEN, G. E. (2014). Climate variability in south-eastern Australia over the last 1500 years inferred from the high-resolution diatom records of two crater lakes. *Quaternary Science Reviews, 95*, 115-131. doi:10.1016/j.quascirev.2014.05.001

BLAAUW, M., VAN GEEL, B., KRISTEN, I., PLESSEN, B., LYARUU, A., ENGSTROM, D. R., . . . VERSCHUREN, D. (2011). High-resolution 14C dating of a 25,000-year lake-sediment record from equatorial East Africa. *Quaternary Science Reviews, 30*(21), 3043-3059. doi:10.1016/j.quascirev.2011.07.014

BOLLHÖFER, A., MANGINI, A., LENHARD, A., WESSELS, M., GIOVANOLI, F., & SCHWARZ, B. (1994). High-resolution 210 Pb dating of Lake Constance sediments: Stable lead in Lake Constance. *International Journal of Geosciences, 24*(4), 267-274. doi:10.1007/BF00767087

BÖRNER, N., DE BAERE, B., YANG, Q., JOCHUM, K. P., FRENZEL, P., ANDREAE, M. O., & SCHWALB, A. (2013). Ostracod shell chemistry as proxy for paleoenvironmental change. *Quaternary International, 313-314*. doi:10.1016/j.quaint.2013.09.041

BOWLER, J. M. (1981). Australian salt lakes - a paleohydrologic approach. *Hydrobiologia, 81*(3), 431-444.

BOWLER, J. M., & TATSUJI, H. (1971). Late Quaternary Stratigraphy and Radiocarbon Chronology of Water Level Fluctuations in Lake Keilambete, Victoria. *Nature, 232*(5309), 330. doi:10.1038/232330a0

BRAGANZA, K., GERGIS, J. L., POWER, S. B., RISBEY, J. S., & FOWLER, A. M. (2009). A multiproxy index of the El Niño–Southern Oscillation, A.D. 1525–1982. *Journal of Geophysical Research, 114*(D5). doi:10.1029/2008jd010896

BRIGHT, J., KAUFMAN, D. S., FORESTER, R. M., & DEAN, W. E. (2006). A continuous 250,000 yr record of oxygen and carbon isotopes in ostracode and bulk-sediment carbonate from Bear Lake, Utah-Idaho. *Quaternary Science Reviews, 25*(17), 2258-2270. doi:10.1016/j.quascirev.2005.12.011

BUREAU OF METEOROLOGY. (2019). Climate statistics for Australian locations. Retrieved from http://www.bom.gov.au/jsp/ncc/cdio/cvg/av?p_stn_num=090035&p_prim_element_index=18&p_display_type=statGraph&period_of_avg=ALL&normals_years=allYearOfData&staticPage=

DE DECKKER, P. (1986). Biological and Sedimentary Facies of Australian Salt Lakes. *Paleogeography, Paleoclimatology, Paleoecology, 62*(1-4), 237-270.

DEAN, J. R., EASTWOOD, W. J., ROBERTS, N., JONES, M. D., YIĞITBAŞIOĞLU, H., ALLCOCK, S. L., . . . LENG, M. J. (2015). Tracking the hydro-climatic signal from lake to sediment: A field study from central Turkey. *Journal of Hydrology, 529*(2), 608-621. doi:10.1016/j.jhydrol.2014.11.004

DECROUY, L., VENNEMANN, T. W., & ARIZTEGUI, D. (2011). Controls on ostracod valve geochemistry: Part 2. Carbon and oxygen isotope compositions. *Geochimica et Cosmochimica Acta, 75*(22), 7380-7399. doi:10.1016/j.gca.2011.09.008

ESPER, J., KRUSIC, P. J., LJUNGQVIST, F. C., LUTERBACHER, J., CARRER, M., COOK, E., . . . BÜNTGEN, U. (2016). Ranking of tree-ring based temperature reconstructions of the past millennium. *Quaternary Science Reviews, 145*, 134-151. doi:10.1016/j.quascirev.2016.05.009

FALSTER, G., DELEAN, S., & TYLER, J. (2018). Hydrogen Peroxide Treatment of Natural Lake Sediment Prior to Carbon and Oxygen Stable Isotope Analysis of Calcium Carbonate. *Geochemistry, Geophysics, Geosystems, 19*(9), 3583-3595. doi:10.1029/2018gc007575

FEDOTOV, A., IGNAT'EV, A., & VELIVETSKAYA, T. (2015). Reconstruction of deglaciation of Northern Mongolia for the last 330 ka BP, inferred from ostracod stable isotope records from Lake Khubsugul. *Environmental Earth Sciences, 74*(3), 2041-2054. doi:10.1007/s12665-015-4283-0

FENG, J., LI, J., LI, Y., ZHU, J., & XIE, F. (2015). Relationships among the monsoon-like southwest Australian circulation, the Southern Annular Mode, and winter rainfall over southwest Western Australia. *Advances in Atmospheric Sciences, 32*(8), 1063-1076. doi:10.1007/s00376-014-4142-z

FREUND, M., HENLEY, B. J., KAROLY, D. J., ALLEN, K. J., & BAKER, P. J. (2017). Multi-century cool- AND warm-season rainfall reconstructions for Australia's major climatic regions. *Climate of the Past, 13*(12), 1751. doi:10.5194/cp-13-1751-2017

GELL, P. A., BARKER, P. A., DE DECKKER, P., LAST, W. M., & JELICIC, L. (1994). The Holocene history of West Basin Lake, Victoria, Australia; chemical changes based on fossil biota and sediment mineralogy. *Journal of Paleolimnology, 12*, 235-258.

GOURAMANIS, C., DE DECKKER, P., SWITZER, A. D., & WILKINS, D. (2013). Cross-continent comparison of high-resolution Holocene climate records from southern Australia — Deciphering the impacts of far-field teleconnections. *Earth-Science Reviews, 121*, 55-72. doi:10.1016/j.earscirev.2013.02.006

GOURAMANIS, C., WILKINS, D., & DE DECKKER, P. (2010). 6000 years of environmental changes recorded in Blue Lake, South Australia, based on ostracod ecology and valve chemistry. *Palaeogeography, Palaeoclimatology, Palaeoecology, 297*(1), 223-237. doi:10.1016/j.palaeo.2010.08.005

HOLMES, J., STREET-PERROTT, F., ALLEN, M., FOTHERGILL, P., HARKNESS, D., KROON, D., & PERROTT, R. (1997). Holocene palaeolimnology of Kajemarum Oasis, Northern Nigeria: an isotopic study of ostracodes, bulk carbonate and organic carbon. *Journal of the Geological Society, 154*(2), 311-319. doi:10.1144/gsjgs.154.2.0311

HOTCHKIS, M., CHILD, D., FROEHLICH, M., WALLNER, A., WILKCKEN, K., & WILLIAMS, M. (2019). Actinides AMS on the VEGA accelerator. *Nuclear Instruments and Methods in Physics Research Section B: Beam Interactions with Materials and Atoms, 438*, 70-76.

JONES, M. D., & DEE, S. G. (2018). Global-scale proxy system modelling of oxygen isotopes in lacustrine carbonates: New insights from isotope-enabled-model proxy-data comparison. *Quaternary Science Reviews, 202*, 19-29. doi:10.1016/j.quascirev.2018.09.009

JONES, M. D., LENG, M. J., ROBERTS, C. N., TÜRKEŞ, M., & MOYEED, R. (2005). A Coupled Calibration and Modelling Approach to the Understanding of Dry-Land Lake Oxygen Isotope Records. *Journal of Paleolimnology, 34*(3), 391-411. doi:10.1007/s10933-005-6743-0

KALM, V., & SOHAR, K. (2010). Oxygen isotope fractionation in three freshwater ostracod species from early Holocene lacustrine tufa in northern Estonia. *Journal of Paleolimnology, 43*(4), 815-828. doi:10.1007/s10933-009-9370-3

LAST, W. M., & DE DECKKER, P. (1990). Modern and Holocene carbonate sedimentology of two saline volcanic maar lakes, southern Australia. *Sedimentology, 37*, 967-981.

LI, H. C., KU, T. L., STOTT, L. D., & ANDERSON, R. F. (1997). Stable isotope studies on Mono Lake (California). 1. δ 18 O in lake sediments as proxy for climatic change during the last 150 years. *Limnology and Oceanography, 42*(2), 230-238. doi:10.4319/lo.1997.42.2.0230

LOCKIER, E. R. (2015). *Hydroclimate variability during the past millennium: a new record from West Basin Lake, Victoria.* (Honours Thesis), The University of Adelaide, Adelaide, Australia.

MARCHEGIANO, M., FRANCKE, A., GLIOZZI, E., & ARIZTEGUI, D. (2018). Arid and humid phases in central Italy during the Late Pleistocene revealed by the Lake Trasimeno ostracod record. *Palaeogeography, Palaeoclimatology, Palaeoecology, 490*, 55-69. doi:10.1016/j.palaeo.2017.09.033

MCCORMACK, J., VIEHBERG, F., AKDEMIR, D., IMMENHAUSER, A., & KWIECIEN, O. (2019). Ostracods as ecological and isotopic indicators of lake water salinity changes: the Lake Van example. *Biogeosciences, 16*(10), 2095-2114. doi:10.5194/bg-16-2095-2019

MISCHKE, S., BÖßNECK, U., DIEKMANN, B., HERZSCHUH, U., JIN, H., KRAMER, A., . . . ZHANG, C. (2010). Quantitative relationship between water-depth and sub-fossil ostracod assemblages in Lake Donggi Cona, Qinghai Province, China. *Journal of Paleolimnology, 43*(3), 589-608. doi:10.1007/s10933-009-9355-2

NICHOLLS, N., & KARIKO, A. (1993). East Australian rainfall events: Interannual variations, trends, and relationships with the Southern Oscillation. *Journal of Climate, 6*(6). doi:10.1175/1520-0442(1993)0062.0.CO
2

O'DONNELL, A. J., COOK, E. R., PALMER, J. G., TURNEY, C. S. M., & GRIERSON, P. F. (2018). Potential for tree rings to reveal spatial patterns of past drought variability across western Australia. *Environmental Research Letters, 13*(2). doi:10.1088/1748-9326/aaa204

PRODAN, H. (2014). *An investigation into the sedimentary laminations at West Basin Lake, Victoria: Are they varves?* (Honours thesis), The University of Adelaide, Adelaide, Australia.

PUI, A., SHARMA, A., SANTOSO, A., & WESTRA, S. (2012). Impact of the El Niño-Southern Oscillation, Indian Ocean Dipole, and Southern Annular Mode on Daily to Subdaily Rainfall Characteristics in East Australia. *Monthly Weather Review, 140*(5), 1665-1682. doi:10.1175/MWR-D-11-00238.1
RICKETTS, R. D., & ANDERSON, R. F. (1998). A direct comparison between the historical record of lake level and the δ 18 O signal in carbonate sediments from Lake Turkana, Kenya. *Limnology and Oceanography, 43*(5), 811-822. doi:10.4319/lo.1998.43.5.0811
RISBEY, J., POOK, M. J., MCINTOSH, P. C., UMMENHOFER, C. C., & MEYERS, G. (2009). Characteristics and variability of synoptic features associated with cool season rainfall in southeastern Australia. *International Journal of Climatology, 29*(11), 1595-1613. doi:10.1002/joc.1775
SADLER, J., NGUYEN, A. D., LEONARD, N., WEBB, G., & NOTHDURFT, L. (2016). Acropora interbranch skeleton Sr/Ca ratios: Evaluation of a potential new high-resolution paleothermometer. *Paleoceanography, 31*(4), 505-517. doi:10.1002/2015PA002898
SANDERS, C. J., SANTOS, I. R., MAHER, D. T., BREITHAUPT, J. L., SMOAK, J. M., KETTERER, M., . . . EYRE, B. D. (2016). Examining (239+240)Pu, (210)Pb and historical events to determine carbon, nitrogen and phosphorus burial in mangrove sediments of Moreton Bay, Australia. *J Environ Radioact, 151*, 623-629. doi:10.1016/j.jenvrad.2015.04.018
STEINMAN, B. A., & ABBOTT, M. B. (2013). Isotopic and hydrologic responses of small, closed lakes to climate variability: Hydroclimate reconstructions from lake sediment oxygen isotope records and mass balance models. *Geochimica et Cosmochimica Acta, 105*, 342-359. doi:10.1016/j.gca.2012.11.027
STEINMAN, B. A., ABBOTT, M. B., MANN, M., E. , STANSELL, N., D. , & FINNEY, B., P. . (2012). 1,500 year quantitative reconstruction of winter precipitation in the Pacific Northwest. *Proceedings of the National Academy of Sciences, 109*(29), 11619. doi:10.1073/pnas.1201083109
STEINMAN, B. A., ROSENMEIER, M. F., ABBOTT, M. B., & BAIN, D. J. (2010). The isotopic and hydrologic response of small, closed-basin lakes to climate forcing from predictive models: Application to paleoclimate studies in the upper Columbia River basin. *Limnology and Oceanography, 55*(6), 2231-2245. doi:10.4319/lo.2010.55.6.2231
TIBBY, J., TYLER, J. J., & BARR, C. (2018). Post little ice age drying of eastern Australia conflates understanding of early settlement impacts. *Quaternary Science Reviews, 202*, 45-52. doi:10.1016/j.quascirev.2018.10.033
TIMMS, B. V. (1972). A Meromicitic Lake in Australia. *Limnology and Oceanography, 17*(16), 918-922.
UMMENHOFER, C. C., ENGLAND, M. H., MCINTOSH, P. C., MEYERS, G. A., POOK, M. J., RISBEY, J. S., . . . TASCHETTO, A. S. (2009). What causes southeast Australia's worst droughts? *Geophysical Research Letters, 36*(4). doi:10.1029/2008gl036801
WILKINS, D., GOURAMANIS, C., DE DECKKER, P., FIFIELD, L. K., & OLLEY, J. (2013). Holocene lake-level fluctuations in Lakes Keilambete and Gnotuk, southwestern Victoria, Australia. *The Holocene, 23*(6), 784-795. doi:10.1177/0959683612471983
ZHANG, X. C., ZHANG, G. H., GARBRECHT, J. D., & STEINER, J. L. (2015). Dating Sediment in a Fast Sedimentation Reservoir using Cesium-137 and Lead-210. *Soil Science Society of America Journal, 79*(3). doi:10.2136/sssaj2015.01.0021
ZHU, Z.-J., CHEN, J.-A., LI, D.-H., REN, S.-C., & LIU, F. (2012). Li/Ca ratios of ostracod shells at Lake Qinghai, NE Tibetan Plateau, China: a potential temperature indicator. *Environmental Earth Sciences, 67*(6), 1735-1742. doi:10.1007/s12665-012-1617-z

9.0 APPENDICES:

9.1 EXTENDED METHODS

Appendices A through D
See files at:
https://universityofadelaide.box.com/s/vhyjrkwoel9p1in7vwlfj7gf59kcvybj
Appendix E

Dry Bulk Density Methods

1. Label 100 mL beakers with the sample IDs and weigh them. Record the masses in the spreadsheet above.
2. Label 25 mL measuring cylinders with the sample IDs. Fill up each measuring cylinders with 20 mL of water. Record the masses (measuring cylinder + 20 mL of water).
3. Transfer at least 2 mL volume of wet sample into the measuring cylinder. If the samples are sticky, avoid touching the wall of the measuring cylinder with the sample. Use a thin plastic pasteur pipette to transfer the sediment into the measuring cylinder. Place the sample on the tip of the pasteuer pipette and insert it into the measuring cylinders all the way into the water. The sample should come off easily from the pipette. Keep adding a small ammout at a time until you have transferred at least 2 mL volume of sample.
4. Record the weight of the measuring cylinder + water + wet sample.
5. Record the volume after you added the sample.
6. Transfer the content of the measuring cylinder (from step 3) into the beaker (from step 1). Rinse the inside of the measuring cylinder with water from a wash bottle. Transfer the rinse into the beaker. Keep rinsing until all the sample from the measuring cylinder has been transferred into the beaker. However, try not to use too much water, otherwise it takes longer to dry the samples.
7. Place the beaker and content in the oven at 60C.
8. Repeat for all other samples.
9. Once the samples have dried up (2-3 days later). Record the dry sample + beaker masses.
10. Calculate dry weight / wet volume (dry bulk density)

9.2 EXTENDED RESULTS

See appendix F at:
https://universityofadelaide.box.com/s/vhyjrkwoel9p1in7vwlfj7gf59kcvybj

Appendix G

Table 3: Results of the Ostracod Calcite IRMS analysis.

Depth (cm)	δ13C (‰ V-PDB)	δ13C error (‰)	δ18O (‰ V-PDB)	δ18O error (‰)	Depth (cm)	δ13C (‰ V-PDB)	δ13C error (‰)	δ18O (‰ V-PDB)	δ18O error (‰)
0.75	-6.29868	0.084116	3.155439	0.204688	8.25	-3.57725	0.070432	2.899695	0.14162
1.25	-4.07737	0.097626	3.037187	0.192641	8.5	-3.16159	0.076582	2.894854	0.202419
1.5	-3.28462	0.045044	2.964227	0.1292	8.75	-3.0549	0.060242	2.948034	0.158603
1.75	-5.61711	0.060752	2.707365	0.095232	9	-3.07652	0.083823	2.819611	0.155436
2	-2.86814	0.05143	2.990156	0.134691	9.25	-2.17533	0.076433	2.814531	0.19853
2.25	-3.73665	0.037338	2.811981	0.175671	9.5	-1.60273	0.105754	2.693093	0.142788
2.5	-2.69682	0.064587	3.0304	0.105417	9.75	-1.37259	0.097333	2.680549	0.161022
2.75	-3.8283	0.03938	3.124751	0.12172	11	-2.85902	0.051652	3.918816	0.060099
3	-2.67942	0.053387	3.884055	0.099144	14	-1.80358	0.044981	3.651529	0.114424
3.25	-2.91323	0.111136	4.381083	0.250764	16	2.465833	0.213456	3.945471	0.275515
3.5	-3.7972	0.028019	4.34935	0.132231	17	-2.0871	0.07155	1.89739	0.028774
3.75	-4.47874	0.117856	4.06088	0.289491	23	0.949709	0.12885	5.621463	0.137636
4	-3.42199	0.078451	4.244458	0.156615	24	3.491496	0.072897	4.562443	0.130607
4.25	-4.38668	0.151334	3.785367	0.220298	27.5	-3.90911	0.052913	3.140688	0.216393
4.5	-2.63283	0.069686	4.609655	0.118509	28	-3.4967	0.074367	3.076059	0.206293
4.75	-4.09394	0.046943	3.865782	0.053719	28.5	-3.30251	0.098228	3.376361	0.260388
5	-2.8915	0.087137	4.205934	0.147723	29	-2.77353	0.089995	3.589338	0.174906
5.25	-5.87781	0.167655	3.721981	0.174323	29.5	-2.61421	0.054463	3.972349	0.146528
5.75	-2.26448	0.171622	3.450942	0.265449	30.5	-1.64892	0.057322	2.930661	0.151106
6	-4.6137	0.191579	3.307426	0.194451	31	-0.08476	0.059618	2.992643	0.125273
6.25	-3.87312	0.087747	3.190225	0.150894	31.5	0.288078	0.040273	3.134777	0.093969
6.5	-3.5022	0.110838	3.378784	0.188076	32	0.43906	0.042959	2.985078	0.124896
6.75	-3.77622	0.123021	3.275872	0.231371	32.5	0.173536	0.026263	3.450492	0.124626
7	-3.29769	0.077052	3.117119	0.204002	36.5	0.203058	0.067436	3.168149	0.132546
7.25	-3.19604	0.074866	3.228833	0.190314	37	-0.67932	0.057707	3.964235	0.117037

Appendix H

Table 4. Results of BIC analysis at room temperature

Depth (cm)	δ13C (‰ PDB)	δ13C error (‰)	δ18O (‰ SMOW)	δ18O error (‰)	Depth (cm)	δ13C (‰ PDB)	δ13C error (‰)	δ18O (‰ SMOW)	δ18O error (‰)
0.75	1.581562	0.135298	3.720037	0.284846	14.5	-1.33178	0.095226	4.581317	0.57766
1.25	1.279735	0.069868	3.684961	0.103935	17.5	1.58122	0.346335	9.141396	0.820492
1.75	1.724986	0.022578	3.439367	0.064402	19	-3.94617	0.087128	-0.55487	0.221362
2	1.601643	0.031071	2.884185	0.088102	20	-0.55777	0.046259	4.828163	0.061339
2.5	0.938286	0.113969	3.809007	0.667189	21	0.286739	0.047549	3.319374	0.135392
3	0.33686	0.196681	2.771954	0.861796	22	1.207142	0.043317	5.070374	0.196694
3.25	1.828079	0.055294	4.277898	0.035216	22.5	1.192059	0.045264	4.661595	0.140581
3.5	1.389207	0.086765	3.10615	0.288103	23	1.672149	0.053772	4.886946	0.141561
3.75	2.489131	0.025515	4.728652	0.06119	23.5	1.642851	0.031991	4.639532	0.06115
4	3.168248	0.056188	5.703417	0.04231	24	1.079832	0.166065	4.046692	0.22814
4.25	2.629287	0.05078	4.964093	0.069515	24.5	1.280308	0.221614	4.686525	0.489486
4.5	4.12896	0.10279	6.777053	0.150943	26	1.371733	0.107089	4.012987	0.153899
4.75	4.462799	0.071474	8.763755	0.154383	26.5	1.473959	0.167925	5.697464	0.340684
5	3.858308	0.075055	7.371542	0.11286	27	0.332007	0.103625	3.530677	0.257259
5.25	-2.24731	0.082821	0.730476	0.207153	27.5	1.692688	0.036875	4.287508	0.198465
5.5	-0.21771	0.026412	2.348124	0.108613	28	2.168486	0.034606	4.538762	0.105381
5.75	-0.38651	0.044449	3.068471	0.066238	28.5	2.385255	0.98929	3.595461	0.153189
6.75	-0.18929	0.112492	3.573124	0.271492	29	1.927287	0.039375	3.860752	0.144672
7	-0.55827	0.072132	3.720427	0.212632	29.5	1.92994	0.024999	-1.38884	0.118485
7.75	-0.85352	0.054008	3.196391	0.070033	30	2.030876	0.022348	3.949135	0.103013
8	-0.33485	0.06233	4.086491	0.177393	30.5	1.861173	0.01217	3.705764	0.087759
8.5	-1.49178	0.050137	2.343038	0.058793	31	1.812461	0.068117	3.57223	0.126185
8.75	-1.70219	0.052341	2.417293	0.132317	31.5	2.648337	0.040649	5.124634	0.092658
9.5	-3.69285	0.186542	-0.02262	0.521372	32	1.858253	0.051916	2.847971	0.11796
11.25	-2.81098	0.118694	3.281794	0.307021	33	2.201343	0.049121	4.729677	0.047007

Appendix I

Table 5. Results of BIC analysis at 70 °C

Depth (cm)	δ13C (‰ PDB)	δ13C error (‰)	δ18O (‰ SMOW)	δ18O error (‰)	Depth (cm)	δ13C (‰ PDB)	δ13C error (‰)	δ18O (‰ SMOW)	δ18O error (‰)
0.75	1.581562	0.135298	3.720037	0.284846	14.5	-1.33178	0.095226	4.581317	0.57766
1.25	1.279735	0.069868	3.684961	0.103935	17.5	1.58122	0.346335	9.141396	0.820492
1.75	1.724986	0.022578	3.439367	0.064402	19	-3.94617	0.087128	-0.55487	0.221362
2	1.601643	0.031071	2.884185	0.088102	20	-0.55777	0.046259	4.828163	0.061339
2.5	0.938286	0.113969	3.809007	0.667189	21	0.286739	0.047549	3.319374	0.135392
3	0.33686	0.196681	2.771954	0.861796	22	1.207142	0.043317	5.070374	0.196694
3.25	1.828079	0.055294	4.277898	0.035216	22.5	1.192059	0.045264	4.661595	0.140581
3.5	1.389207	0.086765	3.10615	0.288103	23	1.672149	0.053772	4.886946	0.141561
3.75	2.489131	0.025515	4.728652	0.06119	23.5	1.642851	0.031991	4.639532	0.06115
4	3.168248	0.056188	5.703417	0.04231	24	1.079832	0.166065	4.046692	0.22814
4.25	2.629287	0.05078	4.964093	0.069515	24.5	1.280308	0.221614	4.686525	0.489486
4.5	4.12896	0.10279	6.777053	0.150943	26	1.371733	0.107089	4.012987	0.153899
4.75	4.462799	0.071474	8.763755	0.154383	26.5	1.473959	0.167925	5.697464	0.340684
5	3.858308	0.075055	7.371542	0.11286	27	0.332007	0.103625	3.530677	0.257259
5.25	-2.24731	0.082821	0.730476	0.207153	27.5	1.692688	0.036875	4.287508	0.198465
5.5	-0.21771	0.026412	2.348124	0.108613	28	2.168486	0.034606	4.538762	0.105381
5.75	-0.38651	0.044449	3.068471	0.066238	28.5	2.385255	0.98929	3.595461	0.153189
6.75	-0.18929	0.112492	3.573124	0.271492	29	1.927287	0.039375	3.860752	0.144672
7	-0.55827	0.072132	3.720427	0.212632	29.5	1.92994	0.024999	-1.38884	0.118485
7.75	-0.85352	0.054008	3.196391	0.070033	30	2.030876	0.022348	3.949135	0.103013
8	-0.33485	0.06233	4.086491	0.177393	30.5	1.861173	0.01217	3.705764	0.087759
8.5	-1.49178	0.050137	2.343038	0.058793	31	1.812461	0.068117	3.57223	0.126185
8.75	-1.70219	0.052341	2.417293	0.132317	31.5	2.648337	0.040649	5.124634	0.092658
9.5	-3.69285	0.186542	-0.02262	0.521372	32	1.858253	0.051916	2.847971	0.11796
11.25	-2.81098	0.118694	3.281794	0.307021	33	2.201343	0.049121	4.729677	0.047007